

jXBW: Fast Substructure Search in Large-Scale JSONL Datasets for Foundation Model Applications

Yasuo Tabei

yasuo.tabei@riken.jp

RIKEN Center for Advanced Intelligence Project
Tokyo, Japan

ABSTRACT

Substructure search in JSON Lines (JSONL) datasets is essential for modern applications such as prompt engineering in foundation models, but existing methods suffer from prohibitive computational costs due to exhaustive tree traversal and subtree matching. We present jXBW, a fast method for substructure search on large-scale JSONL datasets. Our method makes three key technical contributions: (i) a merged tree representation built by merging trees of multiple JSON objects while preserving individual identities, (ii) a succinct data structure based on the eXtended Burrows-Wheeler Transform that enables efficient tree navigation and subpath search, and (iii) an efficient three-step substructure search algorithm that combines path decomposition, ancestor computation, and adaptive tree identifier collection to ensure correctness while avoiding exhaustive tree traversal. Experimental evaluation on real-world datasets demonstrates that jXBW consistently outperforms existing methods, achieving speedups of 16 \times for smaller datasets and up to 4,700 \times for larger datasets over tree-based approaches, and more than 6 \times 10⁶ over XML-based processing while maintaining competitive memory usage.

CCS CONCEPTS

- **Information systems** → **Data structures**; *Query processing*;
- **Theory of computation** → *Data compression*; • **Computing methodologies** → *Machine learning*.

KEYWORDS

XBW Transform, Substructure Search, JSONL, Compressed Data Structure, Foundation Models

ACM Reference Format:

Yasuo Tabei. 2018. jXBW: Fast Substructure Search in Large-Scale JSONL Datasets for Foundation Model Applications. In *Proceedings of Make sure to enter the correct conference title from your rights confirmation email (Conference acronym 'XX)*. ACM, New York, NY, USA, 17 pages. <https://doi.org/XXXXXX.XXXXXXX>

Permission to make digital or hard copies of all or part of this work for personal or classroom use is granted without fee provided that copies are not made or distributed for profit or commercial advantage and that copies bear this notice and the full citation on the first page. Copyrights for components of this work owned by others than the author(s) must be honored. Abstracting with credit is permitted. To copy otherwise, or republish, to post on servers or to redistribute to lists, requires prior specific permission and/or a fee. Request permissions from permissions@acm.org.

Conference acronym 'XX, June 03–05, 2018, Woodstock, NY

© 2018 Copyright held by the owner/author(s). Publication rights licensed to ACM. ACM ISBN 978-1-4503-XXXX-X/2018/06...\$15.00
<https://doi.org/XXXXXX.XXXXXXX>

1 INTRODUCTION

JSON Lines (JSONL) is a widely adopted data format in which each line contains a single, self-contained JSON object. The importance of JSONL has grown significantly with the rise of Foundation Models [4], where structured prompt inputs containing diverse, semi-structured information must be efficiently processed and queried. Foundation Models such as GPT [5, 24], BERT [10], T5 [25], LLaMA [27, 28], and Claude [2] are commonly deployed with JSONL-formatted prompt inputs for tasks including question answering, text generation, and information retrieval, with recent empirical studies demonstrating up to 40 % performance improvements over plain text formats [7] and comparative studies with GPT-4o showing that JSON-formatted inputs achieve the highest accuracy for complex structured data processing compared to YAML or hybrid CSV formats [31]. Enterprise applications and research platforms commonly employ JSONL format to manage complex prompt datasets that can contain millions of structured queries and contextual information [8, 18, 30]. There is therefore a compelling and growing need to develop novel, more powerful methods for effectively utilizing large-scale JSONL datasets to draw out the capabilities of foundation models through prompt engineering.

Substructure search in JSONL data is essential for prompt engineering in foundation models. The goal is to find all JSON objects that contain a given query as a substructure. Each JSON object can be naturally represented as a tree structure, transforming substructure search into a tree matching problem. This problem must handle both ordered structures (JSON arrays) and unordered structures (JSON objects). Simple pointer-based approaches require traversing each JSON tree individually and performing explicit enumeration and comparison of child nodes, making them computationally prohibitive for large-scale datasets. While space-efficient succinct tree representations called SJSON for JSON objects exist [17], they still suffer from the same computational bottlenecks in substructure search tasks.

Alternatively, one can transform JSON objects into XML and leverage XQuery for substructure search, benefiting from mature XML indexing technologies [6, 26]. However, this approach introduces substantial overhead: the JSON-to-XML conversion process increases data volume and processing latency, while semantic differences between JSON and XML models—particularly in handling arrays, null values, and type distinctions—complicate query formulation and result interpretation. Moreover, this approach requires performing individual substructure searches across numerous XML documents converted from each JSON object, leading to computational overhead that scales linearly with dataset size. Additionally, XML indexing techniques cannot exploit the structural similarities commonly found among JSON objects in JSONL datasets, missing

optimization opportunities that are naturally available in JSON-native approaches. Therefore, an important open challenge is to develop specialized data structures and algorithms that can efficiently support substructure search directly on JSONL data.

Contribution. We present jXBW (JSONL eXtended Burrows-Wheeler Transform), a novel approach for fast substructure search on large JSONL datasets that addresses the computational bottlenecks of existing methods through three key innovations:

(1) Merged Tree Representation: We convert each JSON object into a tree structure and merge multiple trees into a single unified merged tree. This representation exploits structural similarities among JSON objects to reduce memory overhead and enables efficient substructure search.

(2) Compressed Tree Index (jXBW): Since pointer-based representations require expensive tree traversal for substructure matching, we introduce jXBW—a compressed representation based on the eXtended Burrows-Wheeler Transform (XBW) for trees [12]. XBW enables efficient tree navigation operations in $O(\log \sigma)$ time, where σ is the alphabet size of distinct node labels in the tree, and supports subpath search queries in $O(|P| \log \sigma)$ time for paths of length $|P|$. Crucially, subpath search can locate matching paths starting from any node, not just the root. This capability enables an efficient substructure search algorithm that avoids exhaustive tree traversal and explicit comparison of child nodes.

(3) Efficient Substructure Search Algorithm on jXBW: We present a fast substructure search algorithm specifically designed for the jXBW representation that operates in three key steps: (i) path decomposition that transforms query trees into root-to-leaf paths and uses jXBW's subpath search to directly locate matching positions, (ii) ancestor computation that identifies common subtree root positions reachable by all query paths through efficient parent operations, and (iii) tree identifier collection that employs an adaptive strategy to automatically select optimal processing approaches based on query characteristics. This three-step approach ensures correctness while avoiding exhaustive tree traversal, where tree identifiers corresponding to JSONL line numbers are computed through precise operations.

Performance: Our adaptive approach achieves $O((p + r) \times d \times \log \sigma + c \times |Q| \times b \times \log \sigma)$ time complexity, where p is the number of root-to-leaf paths in the query tree, r is the number of matching leaf positions, d is the average path depth, c is the number of validated root positions, and b represents the average branching factor for structural matching operations, while using $O(|MT| \log \sigma)$ space, where $|MT|$ is the number of nodes in the merged tree. This significantly improves upon the $O(|MT| \times |Q|)$ complexity of simple tree traversal approaches, where $|Q|$ are the number of nodes in query tree. Experimental evaluation on seven real-world JSONL datasets demonstrates that jXBW consistently outperforms existing methods, achieving speedups of 16 \times for smaller datasets and up to 4,700 \times for larger datasets over tree-based approaches, and more than 6 \times 10⁶ over XML-based processing while maintaining competitive memory usage.

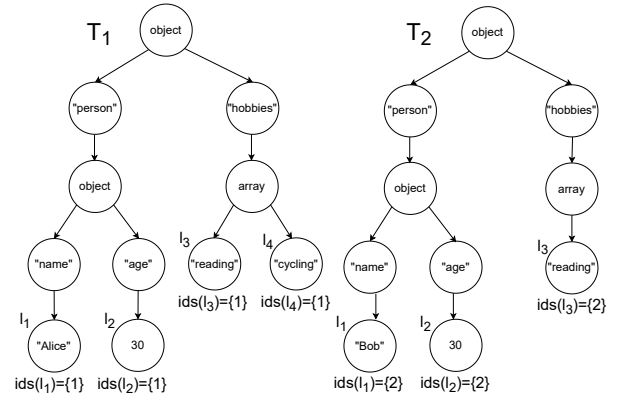


Figure 1: Illustration of tree structures T_1 (left) and T_2 (right), derived from the example JSON objects O_1 and O_2 , respectively.

2 METHOD

2.1 JSONL and its Tree Representation

JSONL is a text-based format in which each line represents a single JSON object composed of key-value pairs. Let a JSONL file consist of N objects denoted by O_i , where $i = 1, 2, \dots, N$. Formally, each JSON object O_i can be defined using Backus–Naur Form (BNF) as follows:

- $\langle \text{object} \rangle ::= \{ \langle \text{members} \rangle ? \}$
- $\langle \text{members} \rangle ::= \langle \text{pair} \rangle (, \langle \text{pair} \rangle)^*$
- $\langle \text{pair} \rangle ::= \langle \text{string} \rangle : \langle \text{value} \rangle$

Here, $\langle \text{value} \rangle$ may be one of the following: $\langle \text{string} \rangle$, $\langle \text{number} \rangle$, $\langle \text{object} \rangle$, $\langle \text{array} \rangle$, true , false , or null .

An $\langle \text{object} \rangle$ may optionally include $\langle \text{members} \rangle$, which consist of one or more unordered $\langle \text{pair} \rangle$ elements. Each $\langle \text{pair} \rangle$ represents a key-value association, where the key is a $\langle \text{string} \rangle$, and the value is any valid JSON data type as defined above. An $\langle \text{array} \rangle$ represents an ordered sequence of elements, each of which may be of any valid JSON data type.

An example involving two JSON objects that manage information about two individuals, Alice and Bob, is given as follows:

```

 $O_1 = \{ \text{"person"} : \{ \text{"name"} : \text{"Alice"}, \text{"age"} : 30, \text{"hobbies"} : [\text{"reading"}, \text{"cycling"}] \}$ 
 $O_2 = \{ \text{"person"} : \{ \text{"name"} : \text{"Bob"}, \text{"age"} : 30, \text{"hobbies"} : [\text{"reading"}] \}$ 

```

Tree Representation. Each object O_i can be systematically transformed into a tree-based representation with node labels. Let T_i denote the tree constructed from the i -th object O_i and $|T_i|$ denote the number of nodes in T_i . The root node of T_i is labeled "object" and has as many unordered child nodes as there are $\langle \text{pair} \rangle$ elements in the $\langle \text{members} \rangle$. If the $\langle \text{object} \rangle$ contains no $\langle \text{members} \rangle$, the root node has no children.

Each $\langle \text{pair} \rangle$ consists of a key-value association of the form $\langle \text{string} \rangle : \langle \text{value} \rangle$. In the corresponding tree structure, each

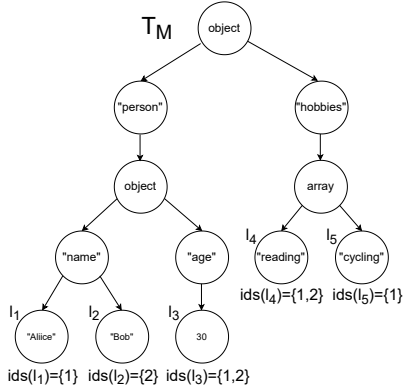


Figure 2: Illustration of the merged tree T_M derived from T_1 and T_2 .

child of the root is labeled with the key `<string>` and has a single child node representing the value. The value node may correspond to any valid JSON type: `<string>`, `<number>`, `<object>`, `<array>`, `true`, `false`, or `null`. If the value is an `<object>`, the tree expands recursively, treating the value node as the root of a new subtree. If the value is an `<array>`, the value node has multiple children, each representing an element of the array in the specified order. Each element may itself be of any valid JSON type.

Furthermore, each leaf node ℓ in tree T_i is annotated with the tree identifier i to track its origin. For any leaf node ℓ , we define $ids(\ell)$ as the set of all tree identifiers associated with that leaf node. In individual trees, this is simply $ids(\ell) = \{i\}$ for leaf node ℓ in tree T_i .

Fig. 1 illustrates the tree structures T_1 and T_2 derived from the example JSON objects O_1 and O_2 which describe two individuals: Alice and Bob. The leaf nodes in T_1 and T_2 are annotated with identifiers 1 and 2, respectively.

Our substructure search is formulated as follows.

Definition 2.1 (Substructure Search Problem). Consider a set of N trees T_1, T_2, \dots, T_N , where each tree T_i is derived from a JSON object in a JSONL file. The substructure search problem is defined as follows: given a query tree Q , find all indices $i \in \{1, 2, \dots, N\}$ such that tree T_i contains Q as a substructure. Here, Q is considered a substructure of T_i if there exists a mapping from each node in Q to a node in T_i such that (i) corresponding nodes have the same label, (ii) the parent-child relationships are preserved, and (iii) the ordering constraints are satisfied according to the JSON semantics: unordered matching for JSON object children and ordered matching for JSON array children.

The query tree Q can be derived from any valid JSON structure: JSON objects, JSON arrays, or nested combinations. The algorithm handles different ordering semantics appropriately:

- JSON objects: unordered matching of key-value pairs
- JSON arrays: ordered matching of elements
- Primitive values: exact value comparison

A naive approach to substructure search in problem 2.1 would involve searching each individual tree T_i separately for the query tree

Q . However, this approach has significant computational drawbacks. First, it requires $O(N \times \sum_{i=1}^N |T_i| \times |Q|)$ time complexity, where $|T_i|$ is the number of nodes in T_i and each tree must be traversed independently to find potential matches. Second, this approach fails to exploit structural similarities between trees, resulting in redundant computations when many trees share common substructures. To overcome these limitations, we introduce an efficient merged tree representation that consolidates shared structural patterns while preserving individual tree identities.

3 MERGED TREE REPRESENTATION

To address these limitations and enable more efficient substructure queries, we construct a single merged tree by combining the individual trees generated from the input JSONL file. Two trees are said to share a common prefix path from the root if their corresponding nodes at each level along the path have identical labels. Nodes that match in both label and position along such a path are merged into a single node in the merged tree MT . When the paths diverge—i.e., when child nodes have different labels—each divergent node continues as a new branch attached to the last shared node on the prefix path.

Each leaf node ℓ in MT retains the identifiers of all individual trees T_i that share the same root-to-leaf path, i.e., $ids(\ell) = \{i \mid T_i \text{ has a leaf node reachable through the same sequence of node labels from root to } \ell\}$. Algorithm 2 in Appendix A presents a pseudo-code for the tree merging algorithm.

An example of the merged tree MT derived from T_1 and T_2 is presented in Fig. 2. In this example, both the leaf nodes labeled “30” and “reading” are reached through paths shared by T_1 and T_2 , resulting in these leaf nodes ℓ_3 and ℓ_4 having $ids(\ell_3) = \{1, 2\}$ and $ids(\ell_4) = \{1, 2\}$ in the merged tree. The other leaf nodes ℓ_1 labeled “Alice”, ℓ_2 labeled “Bob”, and ℓ_5 labeled “cycling” have $ids(\ell_1) = \{1\}$, $ids(\ell_2) = \{2\}$, and $ids(\ell_5) = \{1\}$, respectively.

The merged tree representation provides significant memory efficiency compared to storing individual trees separately. The space complexity of the merged tree is $O(|MT|)$, where $|MT| \leq \sum_{i=1}^N |T_i|$ with equality only when no structural patterns are shared among the input trees. In practice, when input trees share common structural patterns—which is typical in real-world JSONL datasets—the merged tree achieves substantial space savings with $|MT| \ll \sum_{i=1}^N |T_i|$.

When merging a sequence of N trees T_1, T_2, \dots, T_N sequentially, define the total number of nodes as $M_{\text{tot}} = \sum_{i=1}^N |T_i|$. In typical cases where node labels are distinct or only partially overlapping, each merge takes $O(|T| + |T'|)$ time, resulting in a total cost of $O(M_{\text{tot}} \cdot N)$. However, in worst-case scenarios where all node labels are identical and tree structures are highly similar, each individual merge may require $O(|T| \times |T'|)$ time due to the need to examine all possible node pairings, leading to a total cost that can reach $O(M_{\text{tot}}^2)$.

Divide-and-Conquer Strategy. To address this, we adopt a divide-and-conquer strategy that merges trees in a balanced hierarchical manner. At each level of recursion, trees are paired and merged in parallel, and this process is repeated until a single tree remains. Since the total number of nodes M_{tot} remains unchanged throughout the merging process, and each level processes all nodes

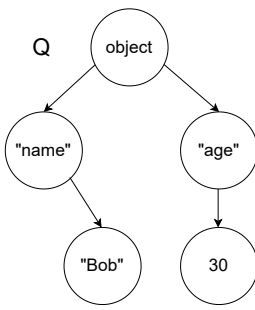


Figure 3: Example query tree structure.

once, the cost per level is $O(M_{\text{tot}})$. As the number of levels is $O(\log N)$, the overall merging cost is reduced to $O(M_{\text{tot}} \log N)$. This strategy significantly improves efficiency by avoiding the accumulation of large intermediate trees that occurs in sequential merging, and it ensures better scalability when handling a large number of input trees.

3.1 Substructure Search on Merged Tree

The substructure search algorithm on the merged tree MT operates as follows. The algorithm operates by traversing MT and identifying candidate nodes with the same label as the root of query tree Q . For each candidate node v , the algorithm recursively verifies whether the subtree rooted at v contains a substructure that matches Q .

The matching process works as follows:

- (1) **Candidate finding:** Finding nodes in MT with the same label as the root of Q by traversing MT .
- (2) **Substructure matching:** For each candidate node v , recursively check if the subtree rooted at v matches the structure of query tree Q . This requires exhaustively comparing the labels of child nodes between corresponding nodes in MT and Q to find matches, resulting in computational overhead that is proportional to the product of the branching factors of both the merged tree and query tree nodes. When the search reaches the j -th leaf node ℓ_j of Q with L leaf nodes, collect the stored tree identifiers from the corresponding matched leaf node in MT and record them in the set $I(\ell_j)$.
- (3) **Solution identification:** Compute the intersection of all collected identifier sets $\bigcap_{j=1}^L I(\ell_j)$ for all leaves $\ell_1, \ell_2, \dots, \ell_L$ in Q . This intersection represents the set of original trees that contain Q as a substructure.

Since each leaf node in the merged tree retains the identifiers of all original trees that contributed to that specific structural path, this approach can identify all trees containing the query as a substructure by leveraging the consolidated structure without requiring individual searches on each original tree.

The detailed algorithms for substructure search on merged tree are provided in Appendix B.

For the example query object `{"name" : "Bob", "age" : 30}`, we convert this object into the tree structure Q as shown in Fig. 3. The algorithm searches for nodes labeled "Object" by recursively

traversing MT in Fig. 2 during the candidate finding phase. It finds root and internal nodes labeled "Object" in MT , and recursively checks whether the subtree rooted at each node matches the structure of Q during the substructure matching phase. One subtree rooted at an internal node labeled "Object" is found to match the structure of Q . The sets of identifiers $I(\ell_2) = \{2\}$ and $I(\ell_3) = \{1, 2\}$ associated with the leaves ℓ_2 and ℓ_3 in MT are collected. In the solution identification phase, we compute the intersection of all collected identifier sets as $I(\ell_2) \cap I(\ell_3) = \{2\} \cap \{1, 2\} = \{2\}$. Thus the solution IDs are $\{2\}$.

Complexity. The substructure search algorithm on the merged tree has significant efficiency limitations. The time complexity is $O(|MT| \times |Q|)$ in the worst case. This occurs when the algorithm must examine every node in MT as a potential starting point for matching the root of Q , and for each candidate node, recursively compare the entire structure of Q against the corresponding subtree in MT . Furthermore, during the substructure matching phase, for each pair of nodes (one from the substructure in MT and one from Q), the algorithm must exhaustively search through all children of the MT node to find those with matching labels to the children of the Q node. Although this approach is more efficient than individual searches on each of the N original trees (which would require $O(N \times \sum_{i=1}^N |T_i| \times |Q|)$ time), the need to traverse the entire merged tree remains a computational bottleneck, especially for large JSON datasets with complex tree structures. To overcome these efficiency limitations and enable fast substructure queries on large-scale data, we present an efficient substructure search algorithm based on jXBW in the following sections.

4 RANK AND SELECT DICTIONARIES

Rank and select dictionary [13, 15, 21] is a data structure for a bit array B , and it is a building block for jXBW. It supports rank and select operations:

- $\text{rank}_c(B, i)$: returns the number of occurrences of $c \in \{0, 1\}$ in $B[1, i]$.
- $\text{select}_c(B, i)$: returns the position of the i -th occurrence of c in B .

Here, $B[1, i]$ denotes the subarray of B from the first to the i -th element.

The rank and select dictionary achieves $O(1)$ query time for both $\text{rank}_c(B, i)$ and $\text{select}_c(B, i)$ operations after preprocessing. The data structure can be constructed in $O(|B|)$ time, where $|B|$ is the length of the bit array B . The space complexity is $|B| + o(|B|)$ bits, where the $|B|$ bits represent the original bit array B , and the $o(|B|)$ bits are used for auxiliary index structures that enable the constant-time operations. In practice, typical implementations require an additional space overhead of approximately 25% to 37.5% of the input size, depending on the specific data structure design and optimization techniques employed [13].

4.1 Wavelet Tree and Matrix

For a general alphabet Σ of size $\sigma = |\Sigma|$, wavelet tree [11, 14, 20] is a succinct data structure that enables efficient rank and select operations on arrays with elements over large alphabets. The key idea is to reduce queries on a large alphabet to a series of binary queries,

which can be answered efficiently using rank and select on bit arrays. Consider a simple example: array $A = [a, b, a, c]$ with elements from alphabet $\{a, b, c\}$. The wavelet tree splits the alphabet into $\{a\}$ and $\{b, c\}$, creating the bit array $[0, 1, 0, 1]$ (where 0 means 'a' and 1 means 'b' or 'c'). To count how many times a appears in the first three positions, we simply compute $\text{rank}_0([0, 1, 0, 1], 3) = 2$. This transforms an element-counting problem into a simple bit-counting problem, which can be solved efficiently using rank operations on bit arrays.

When the tree is balanced, the operations rank_c , select_c , and access can be performed in $O(\log \sigma)$ time. The operation $\text{access}(A, i)$ is also supported and retrieves the element at position i in the array A by following a path from the root to a leaf, guided by the bit array at each level. Given an array A with elements from alphabet Σ , the wavelet tree can store A in $|A|H_0(A) + o(|A| \log \sigma)$ bits, where $H_0(A)$ is the zero-order empirical entropy of A .

The wavelet matrix [9] is an alternative representation that improves upon the wavelet tree by a more cache-friendly and practical layout, while maintaining the same theoretical complexity. Unlike the tree-based structure, the wavelet matrix stores all bit arrays in a matrix form where each level of the original tree becomes a row in the matrix. This representation eliminates the need for explicit tree navigation and reduces memory overhead, making it particularly suitable for large-scale applications. For the XBW representation of merged tree MT described in the next section, we employ the rank and select dictionary and the wavelet matrix to achieve efficient navigation and querying.

5 JXBW

The eXtended Burrows-Wheeler Transform (XBW) [12] is a compressed data structure for labeled trees. The key insight of XBW is to linearize tree structures while preserving their topological properties, enabling (i) efficient navigation operations such as moving from a parent to its children and vice versa and (ii) subpath search operations that can locate matching paths starting from any node. We refer to the XBW representation of MT as jXBW. This specialized application of XBW to our merged tree derived from JSONL data provides a compact representation that supports fast substructure search without explicitly storing the entire tree structure.

5.1 jXBW Construction Process

The construction of the XBW representation for our merged tree MT follows a systematic process as illustrated in Fig. 4.

Step 1: Symbol Table Creation and Label Normalization. Since MT contains diverse node labels from the original JSONL objects (e.g., field names like "name", "age", string values like "Alice", "Bob"), we first establish a symbol table that creates a bijective mapping from each unique node label to a symbol in a unified alphabet Σ (Fig. 4(I)). This mapping enables efficient lexicographic comparison by replacing potentially long string labels with compact symbols.

Using this mapping, all node labels in MT are converted to the standardized alphabet Σ (Fig. 4(II)). Let MT' denote the merged tree with normalized labels and lexicographically sorted children.

Step 2: Array Construction via DFS Traversal. The XBW representation consists of five synchronized arrays (collectively referred to as jXBW arrays), each of length $|MT|$, constructed via a depth-first traversal of MT' (Fig. 4(III)):

- $A_{label}[i]$: stores the label of the i -th visited node during DFS traversal.
- $A_{anc}[i]$: stores the sequence of node labels on the path from the root to the parent of the i -th visited node. For the root node, $A_{anc}[1] = \epsilon$ (empty string).
- $A_{last}[i]$: a binary array where $A_{last}[i] = 1$ if the i -th visited node is the rightmost child of its parent, and 0 otherwise. For the root, $A_{last}[1] = 1$.
- $A_{leaf}[i]$: a binary array where $A_{leaf}[i] = 1$ if the i -th visited node is a leaf, and 0 otherwise.
- $A_{ids}[i]$: stores the set of identifiers ids associated with the i -th visited node.

Step 3: Lexicographic Sorting. All five arrays A_{label} , A_{anc} , A_{last} , A_{leaf} , and A_{ids} are simultaneously sorted based on the lexicographic order of the sequences in A_{anc} (Fig. 4(IV)). In addition, the array A_{label} is indexed by the wavelet matrix. The binary arrays A_{last} and A_{leaf} are also indexed by the rank and select dictionary.

To reduce memory usage, A_{ids} is compacted to contain only entries corresponding to leaf nodes, arranged consecutively without gaps. For a leaf node at array position i , its tree identifiers are accessed via $A_{ids}[\text{rank}_1(A_{leaf}, i)]$, where the rank operation maps the leaf position to the corresponding index in the compacted array.

The resulting arrays, excluding A_{anc} , constitute the XBW representation of MT , which provides a compressed representation that maintains the essential structural information enabling tree navigation operations and a subpath search query while reducing space requirements compared to the explicit tree representation. Note that array A_{anc} is not included in the final XBW representation, but is used only during the construction process. Thus, the space complexity of jXBW is $O(|MT| \log \sigma)$. While this may be comparable to the pointer-based representation $O(|MT'| \log |MT'|)$ in terms of space complexity for JSONL datasets with large vocabularies, jXBW provides significant advantages in query performance.

An important property of the jXBW representation is that (i) siblings are contiguously stored in arrays in lexicographic order of their labels; (ii) the element in A_{last} corresponding to the rightmost child is always 1. These properties are ensured by the XBW construction process: (a) the depth-first traversal of MT' ; (b) the stable lexicographic sorting based on A_{anc} ; (c) the binary encoding in A_{last} , where each sibling block is encoded as a sequence of 0s terminated by a 1 for the rightmost child.

For example, in Fig. 4, the contiguous ranges of array positions of siblings for nodes labeled 'A' (root), 'A' (internal), 'B', 'C', 'F', 'G', 'T' are [2,3], [4,5], [6], [7,8], [9], [10], [11,12], respectively. Array positions 3, 5, 6, 8, 9, 10, 12, which correspond to the rightmost child of each node, are marked as 1 in A_{last} .

5.2 Operations on jXBW

jXBW supports five operations on MT' as follows:

- **Children(i)**: Returns the range $[l, r]$ of positions that represent all children of the node at position i .

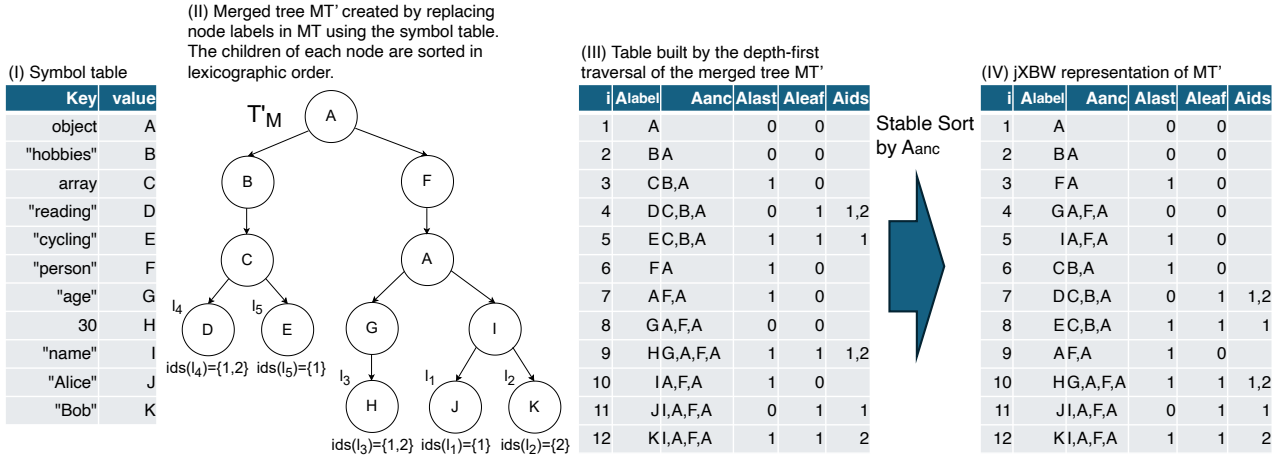


Figure 4: Illustration of the construction process of the XBW representation of the merged tree MT' . Note array A_{anc} is not included in the final jXBW representation and is displayed for clarity.

- **RankedChild**(i, k): Returns the position corresponding to the k -th child of the node at position i in lexicographic order;
- **CharRankedChild**(i, c, k): Returns the position of the k -th child of the node at position i that has label c ;
- **Parent**(i): Returns the position of the parent of the node at position i ;
- **TreeIDs**(i): Returns the set of tree identifiers for leaf node at position i ;
- **SubPathSearch**(P): Returns the range $[l, r]$ of positions that correspond to nodes reachable through path $P = \langle p_1, p_2, \dots, p_k \rangle$;

The detailed algorithms, implementation details, and worked examples for each operation are provided in Appendix C. This subsection presents a conceptual overview of each operation with illustrative examples to facilitate understanding of our substructure search algorithm, which is presented in the next section.

These operations enable efficient navigation through the merged tree structure: **Children** identifies all children of a given node by returning their position range. For example, in Fig. 4, **Children**(5) returns [11, 12] for node labeled 'T', corresponding to children labeled 'J' and 'K'. **RankedChild** provides access to the k -th child in lexicographic order. For instance, **RankedChild**(5, 1) returns position 11 (node labeled 'J'), the first child of node labeled 'T'. **CharRankedChild** selects the k -th child with a specific label. For example, **CharRankedChild**(5, 'K', 1) returns position 12, the first (and only) child labeled 'K' of node labeled 'T'. **Parent** provides upward traversal by returning the parent position. For instance, **Parent**(11) returns position 5, indicating that node labeled 'T' is the parent of node labeled 'J'.

TreeIDs returns the tree identifiers associated with a leaf node. For example, **TreeIDs**(12) returns the set of tree IDs for leaf node labeled 'K', computed efficiently using $A_{ids}[\text{rank}_1(A_{leaf}, 12)]$ where $A_{leaf}[12] = 1$. Since A_{ids} stores only leaf node identifiers in a gap-free manner, this rank-based indexing provides direct access while minimizing memory overhead.

The time complexity of the tree navigation operations (**Children**, **RankedChild**, **Parent**) is $O(\log \sigma)$. **TreeIDs** operates in $O(1)$ time using the rank and select dictionary on A_{leaf} .

SubPathSearch extends these primitives to find all positions of nodes reachable through a given label sequence, enabling efficient pattern matching within the tree structure. For example, for path $P = \langle 'A', 'T' \rangle$, **SubPathSearch**(P) returns [11, 12] on jXBW, which is the range of positions for all nodes reachable through path 'A' \rightarrow 'T'. A key advantage of **SubPathSearch** is that it can find all the paths starting from any node (not only the root), matching a query label sequence P in $O(|P| \log \sigma)$ time. These efficient operations form the foundation for our substructure search algorithm on jXBW, which is presented in the next section.

6 SUBSTRUCTURE SEARCH ALGORITHM ON JXBW

We present an efficient substructure search algorithm that leverages the jXBW representation to achieve significant performance improvements over traditional approaches.

Our jXBW-based substructure search algorithm (Algorithm 1) addresses the fundamental limitations of the merged tree approach through strategic algorithmic approaches.

The key insight behind our approach is to decompose the complex tree matching problem into simpler path matching problems, thereby addressing both inefficiencies of the merged tree method through the following strategies:

Addressing the exhaustive tree traversal problem: Instead of traversing the entire merged tree to find candidate nodes matching the query root label, our algorithm decomposes the query tree Q into all possible root-to-leaf paths and uses **SubPathSearch** to directly locate leaf positions that match each path. By tracing back from these leaf positions using **Parent** operations, we can identify common ancestors that serve as potential subtree roots without exhaustive tree traversal.

Algorithm 1 SubstructureSearch algorithm on jXBW with adaptive processing

```

1: function SUBSTRUCTURESEARCH( $jXBW, Q$ )
   > Step 1: Path Decomposition and Path Matching
2:    $paths \leftarrow$  all root-to-leaf label paths in  $Q$ 
3:    $ranges \leftarrow \emptyset$ 
4:   for  $P \in paths$  do
5:      $[first, last] \leftarrow$  SUBPATHSEARCH( $P$ )
6:      $ranges \leftarrow ranges \cup [first, last]$ 
7:   end for

   > Step 2: Finding common subtree root positions
8:    $ancestor\_sets \leftarrow \emptyset$ 
9:   for  $i = 1$  to  $|paths|$  do
10:     $[first, last] \leftarrow ranges[i]$ 
11:     $ancestor\_sets \leftarrow ancestor\_sets \cup$ 
12:    COMPANCESTORS( $[first, last], paths[i]$ )
13:   end for
14:    $root\_positions \leftarrow \bigcap_{ancestor \in ancestor\_sets} ancestor$ 

   > Step 3: Adaptive tree identifier collection
15:    $all\_matching\_trees \leftarrow \emptyset$ 
16:   for  $root\_pos \in root\_positions$  do           > Use structural
17:     if  $Q$  contains array nodes then           matching for array queries
18:        $struct\_id\_sets \leftarrow$  STRUCTMATCH( $root\_pos, Q.root$ )           ←
19:        $tree\_ids\_for\_this\_root \leftarrow \bigcap_{ids \in struct\_id\_sets} ids$ 
20:     else > Use path-based collection for non-array queries
21:        $path\_id\_sets \leftarrow$  COLLECTPATHMATCHINGIDS( $root\_pos, paths$ )           ←
22:        $tree\_ids\_for\_this\_root \leftarrow \bigcap_{ids \in path\_id\_sets} ids$ 
23:     end if
24:      $all\_matching\_trees \leftarrow all\_matching\_trees \cup$ 
25:      $tree\_ids\_for\_this\_root$ 
26:   end for
27:   return  $all\_matching\_trees$ 
28: end function

```

Addressing explicit child node matching and array ordering constraints: Rather than explicitly enumerating and comparing child nodes during substructure matching, our algorithm employs an adaptive approach that automatically selects the optimal strategy based on query characteristics. For queries containing arrays, the algorithm uses structural matching via **StructMatch** (Algorithm 11), which directly enforces ordering constraints through **CharRankedChild** operations and position-based filtering. For queries without arrays, the algorithm uses path-based processing via **CollectPathMatchingIDs**, which precisely navigates from validated root positions through query paths using efficient jXBW operations. This adaptive strategy ensures correctness while avoiding exhaustive child node enumeration and comparison that characterizes the merged tree approach.

Algorithm 1 implements these strategies through three key steps:

Step 1: Path Decomposition and Path Matching. The algorithm begins by decomposing the query tree Q into all possible

root-to-leaf label paths $paths$. This decomposition transforms the complex tree matching problem into a collection of simpler path matching problems. For each path $P \in paths$, the algorithm applies the **SubPathSearch** operation (Algorithm 8) to identify the position range $[first, last]$ in the jXBW representation that correspond to leaf nodes reachable through that specific path P . This obtains a set of ranges $ranges$, where each range in $ranges$ corresponds to a path in $paths$.

For example, consider the query tree Q in Fig. 3. The path decomposition for Q results in $paths = \{\langle object, "name", "bob" \rangle, \langle object, "age", 30 \rangle\}$, which are converted to $paths = \{\langle A, I, K \rangle, \langle A, G, H \rangle\}$ using the SymbolTable in Fig. 4. Then, the **SubPathSearch** operation is applied to each path $P \in paths$, resulting in $ranges = \{[12, 12], [10, 10]\}$.

Unlike the merged tree approach that requires exhaustive tree traversal, **SubPathSearch** directly locates matching positions in $O(|P| \log \sigma)$ time. The collection of all such ranges, denoted as $ranges$, provides the foundation for subsequent ancestor analysis.

Step 2: Finding common subtree root positions reachable by all query paths. This step identifies positions that can serve as roots for subtrees containing the complete query structure. For each range $[first, last] \in ranges$ computed from path $P \in paths$, the algorithm performs **CompAncestors** (Algorithm 9) to trace back $|P| - 1$ levels using **Parent** operations starting from each position in the range, collecting all ancestor positions that are exactly $|P| - 1$ levels above the leaf positions. All ancestor sets from different paths are collected in $ancestor_sets$. Finally, $root_positions$ contains only those positions that are reachable by all query paths, computed as the intersection of all ancestor sets: $root_positions = \bigcap_{ancestor \in ancestor_sets} ancestor$.

For $ranges = \{[12, 12], [10, 10]\}$, the algorithm computes the ancestors of positions 12 and 10 by going up $|P| - 1 = 3 - 1 = 2$ levels using **Parent** operations for paths $\langle A, I, K \rangle$ and $\langle A, G, H \rangle$. Specifically, for position 12: **Parent**(12) = 5 and **Parent**(5) = 9. For position 10: **Parent**(10) = 4 and **Parent**(4) = 9. The algorithm collects $ancestor_sets = \{\{9\}, \{9\}\}$ from the two paths. The intersection of all ancestor sets yields $root_positions = \{9\} \cap \{9\} = \{9\}$.

Step 3: Adaptive tree identifier collection. For each validated root position $root_pos \in root_positions$, the algorithm adaptively selects the appropriate collection strategy based on the query structure. For queries containing array nodes, the algorithm employs **StructMatch** (Algorithm 11) to perform direct structural matching that inherently handles array ordering constraints. For queries without arrays, the algorithm uses **CollectPathMatchingIDs** (Algorithm 10) which efficiently navigates through query paths using **CharRankedChild** operations. Both approaches ensure precision by starting from each specific $root_pos$ and collecting tree identifiers only from leaves that are actually reachable from that root. The intersection of tree identifier sets from all matched components ensures that only trees containing the complete query structure from the current root are included. The final result aggregates tree identifiers from all valid subtree roots using set union: $all_matching_trees = all_matching_trees \cup tree_ids_for_this_root$.

For $root_positions = \{9\}$, the algorithm processes the single validated root position 9. The **CollectPathMatchingIDs** function is called with $root_pos = 9$ and $paths = \{\langle A, I, K \rangle, \langle A, G, H \rangle\}$. Starting from position 9, the function navigates each path: for path $\langle A, I, K \rangle$,

it follows the sequence of **CharRankedChild** operations to reach leaf position 12, collecting **TreeIDs**(12) = {2}; for path $\langle A, G, H \rangle$, it reaches leaf position 10, collecting **TreeIDs**(10) = {1, 2}. The intersection of {2} and {1, 2} is {2}, setting *tree_ids_for_this_root* = {2}. Finally, *tree_ids_for_this_root* is added to *all_matching_trees*, resulting in *all_matching_trees* = {2}.

Time Complexity Analysis. The adaptive jXBW-based substructure search algorithm achieves significant computational improvements over the merged tree approach. Let p denote the number of root-to-leaf paths in query tree Q , d be the average path depth, σ the alphabet size of distinct node labels, r be the total number of matching leaf positions across all paths (i.e., $r = \sum_{i=1}^p |\text{ranges}[i]|$), and c be the number of validated root positions. The overall time complexity is $O((p+r) \times d \times \log \sigma + c \times |Q| \times b \times \log \sigma)$ where b represents the average branching factor for structural matching operations. This complexity breaks down as follows: (1) Step 1 performs p **SubPathSearch** operations, each taking $O(d \times \log \sigma)$ time, resulting in $O(p \times d \times \log \sigma)$ total time; (2) Step 2 executes $r \times (d-1)$ **Parent** operations for ancestor computation, each taking $O(\log \sigma)$ time, contributing $O(r \times d \times \log \sigma)$; (3) Step 3 adaptively uses either **CollectPathMatchingIDs** for non-array queries ($O(c \times p \times d \times \log \sigma)$) or **StructMatch** for array queries ($O(c \times |Q| \times b \times \log \sigma)$). The structural matching approach handles array ordering constraints directly without post-processing, eliminating false positives. In contrast, the merged tree approach requires $O(|MT| \times |Q|)$ time due to exhaustive tree traversal and explicit child node matching. For large datasets where $|MT| \gg (p+r) \times d \times \log \sigma$, the adaptive jXBW approach provides substantial performance gains while ensuring correctness for all query types, as demonstrated in the experimental evaluation.

7 EXPERIMENTS

7.1 Setup

In this section, we demonstrate the effectiveness of jXBW's substructure search with large JSONL datasets. We used seven datasets, as shown in Table 1. These datasets were obtained from various publicly accessible sources and converted to JSONL format for our experiments. The datasets span diverse domains including entertainment, transportation, government services, geographical information, and chemical compounds, providing a comprehensive evaluation of our jXBW approach across different data characteristics and structural complexities.

"movies" consists of 36,273 movie records scraped from Wikipedia [23] with basic metadata such as titles, years, cast, and genres, containing 9 different key types, and the records are converted into tree structures with an average tree depth of 2.99. "electric_vehicle_population" is a dataset of 247,344 electric vehicle registration records obtained from Kaggle [3] with 28 different key types, represented as tree structures with an average depth of 2.00. "border_crossing_entry" is a dataset of 401,566 border crossing records obtained from Kaggle [1] with tree structures of average depth 2.00, containing a single key type. "mta_nyct_paratransit" consists of 1,572,461 paratransit service records obtained from the U.S. Government data catalog [29], where the service records are converted to tree structures with an average depth of 2.00. "osm_data_newyork" and "osm_data_tokyo" are datasets of 1,090,245 and 6,602,928 OpenStreetMap geographical

objects respectively [22], with 2,001 and 2,496 unique key types. When converted to tree structures, the geographical objects have variable tree depths with averages of 2.47 and 2.36 respectively. "pubchem" consists of 1,000,000 chemical compound records with tree structures of average depth 6.00, where the structural and property information about molecular compounds was obtained from the PubChem database [19]. The original SDF (Structure Data File) format was converted to JSONL format. Each compound is represented as a tree with 53 different types of nodes representing various chemical properties and molecular characteristics.

For query generation, we randomly sampled 1,000 substructures as queries from each dataset, ensuring that each query substructure appears at least once in the corresponding dataset. This approach guarantees that all queries have non-empty result sets and provides realistic evaluation scenarios for substructure search performance. Query substructures were extracted as connected subtrees from the original tree structures, with depths ranging from 2 to 4 nodes to represent typical search patterns. These queries correspond to both JSON object patterns (starting with '{') and JSON array patterns (starting with '['), reflecting the diverse structural patterns found in real-world JSONL data.

We compared jXBW with the following methods. **Ptree** is a merged tree representation using pointers. The JSONL dataset is converted to tree structures and merged into a single merged tree as introduced in Section 3, implemented using standard pointer-based data structures. **SucTree** is a succinct representation based on the approach by Lee et al. [17]. In Lee et al.'s approach, each individual JSON object is represented using a succinct data structure called LOUDS [15] for trees. We extended this idea to represent the merged tree using LOUDS. Both Ptree and SucTree perform substructure search by traversing the merged tree structure as described in Section 3.1.

Saxon [16] is a high-performance XQuery processor widely used in enterprise applications, providing a mature implementation of XQuery 3.1 and XPath 3.1 standards. We used Saxon-HE (Home Edition), the open-source version of Saxon, which provides full XQuery and XSLT processing capabilities. For Saxon-based comparison, we first converted each JSONL dataset to XML format, then performed equivalent substructure searches using XQuery expressions that match the tree patterns used in our jXBW queries. This approach represents the current state-of-the-art for structured document querying in production systems.

We implemented jXBW, Ptree, and SucTree in C++, while Saxon is implemented in Java. We used the C++ SDSL lite library [13] for rank and select dictionary and wavelet matrix in jXBW and SucTree. All experiments were performed on an Apple M4 Max chip with 16-core CPU, 40-core GPU, and 128GB unified memory. Each experiment utilized a single CPU core and a single thread to ensure fair comparison across all methods. We stopped the execution of each method if it had not finished within 24 hours in the experiments.

7.2 Experimental Results

Our experimental evaluation demonstrates the superior performance of jXBW across three critical dimensions: query execution time, memory efficiency, and index construction overhead. The

Table 1: Summary of the JSONL datasets

Dataset	File Size (MB)	#Objects	#Key Types	Avg. Tree Depth	Array Queries (%)
movies	22	36,273	9	2.99	0.0
electric_vehicle_population	199	247,344	28	2.00	0.0
border_crossing_entry	104	401,566	1	2.00	100.0
mta_nyct_paratransit	242	1,572,461	1	2.00	100.0
osm_data_newyork	318	1,090,245	2,001	2.47	0.0
osm_data_tokyo	1,100	6,602,928	2,496	2.36	0.0
pubchem	7,066	1,000,000	53	6.00	0.0

Table 2: Average substructure search time per query in milliseconds

Dataset	Avg Hits	jXBW	Ptree	SucTree	Saxon
movies	70.7	0.016 ± 0.020	0.265 ± 0.025	2.054 ± 0.083	3.958 ± 0.962
electric_vehicle_population	418.6	0.038 ± 0.014	1.278 ± 0.037	10.264 ± 0.276	40.224 ± 7.729
border_crossing_entry	1.0	0.054 ± 0.076	1.407 ± 0.035	13.664 ± 0.579	49.958 ± 6.235
mta_nyct_paratransit	1.0	0.034 ± 0.049	5.619 ± 0.173	48.716 ± 1.447	167.929 ± 23.793
osm_data_newyork	16.4	0.022 ± 0.009	12.464 ± 0.421	97.739 ± 2.553	269.580 ± 18.400
osm_data_tokyo	26.8	0.026 ± 0.012	73.127 ± 1.246	373.371 ± 6.556	1,954.94 ± 72.68
pubchem	268.6	0.043 ± 0.018	26.453 ± 0.692	205.189 ± 6.943	<i>N/A</i>

Table 3: Memory Usage Comparison (in megabytes)

Dataset	SymbolTable	jXBW	Ptree	SucTree	Saxon
movies	48	56	66	50	329
electric_vehicle_population	118	172	219	147	1,664
border_crossing_entry	150	206	255	182	1,593
mta_nyct_paratransit	509	691	875	594	3,241
osm_data_newyork	541	842	1,153	624	4,180
osm_data_tokyo	1,753	2,964	4,264	2,072	8,495
pubchem	2,758	3,880	4,702	3,453	64,840

Table 4: Index Construction Time Comparison (in seconds)

Dataset	Individual Tree Structures	Merging Tree	jXBW	Ptree	SucTree	Saxon
movies	0.162	1.537	1.845	1.821	1.973	0.787
electric_vehicle_population	2.239	155.792	159.066	158.335	159.071	9.599
border_crossing_entry	1.102	355.993	358.634	359.722	362.992	13.169
mta_nyct_paratransit	2.815	4,827.064	4,835.966	5,059.798	5,053.181	55.093
osm_data_newyork	7.548	1,745.005	1,758.649	1,759.208	1,759.115	63.900
osm_data_tokyo	27.592	47,211.042	47,273.986	46,668.465	46,496.468	90.073
pubchem	223.123	15,836.927	16,097.010	16,320.957	15,856.235	629.764

results consistently show that jXBW significantly outperforms all baseline methods across diverse datasets ranging from small movie collections to large-scale chemical compound databases.

Query Performance: Table 2 presents the substructure search performance comparison, where jXBW measurements represent complete end-to-end search time. As shown in Table 1, border_crossing_entry processes queries on the pubchem dataset (1M compounds) in just

and mta_nyct_paratransit consist entirely of queries containing array objects, while the other datasets contain no array queries. jXBW achieves remarkable speedups, consistently delivering the fastest query response times across all datasets. The performance advantage is particularly pronounced for larger datasets: jXBW

0.043 \pm 0.018 milliseconds, while Ptree requires 26.453 \pm 0.692 milliseconds, SucTree takes 205.189 \pm 6.943 milliseconds. Saxon did not finish within 24 hours for the pubchem dataset. This represents speedups of over 615 \times compared to Ptree, 4,772 \times compared to SucTree, and over 6 \times 10⁶ compared to Saxon for complex chemical data queries. Remarkably, even for datasets with 100% array queries (border_crossing_entry, mta_nyct_paratransit), jXBW with structural matching achieves exceptional performance: 26 \times and 165 \times speedups over Ptree, and 253 \times and 1,434 \times speedups over SucTree respectively. The automatic strategy selection demonstrates optimal performance across different query types: structural matching efficiently handles array ordering constraints for array-containing queries.

Memory Efficiency: Table 3 shows the memory usage comparison for index structures. The memory consumption of jXBW, Ptree, and SucTree includes the symbol table overhead, which represents the dominant component of memory usage for these tree-based methods. jXBW maintains competitive memory usage: SucTree achieves the most aggressive compression, while jXBW's memory overhead remains significantly lower than both Ptree and Saxon across most datasets. For instance, on the osm_data_tokyo dataset, jXBW uses 2,964 MB compared to Ptree's 4,264 MB and Saxon's 8,495 MB. jXBW with fast substructure search provides efficient memory utilization through rank and select operations on compressed bit arrays and wavelet matrices, making jXBW particularly attractive for large-scale applications.

Construction Time: Table 4 shows the construction time breakdown including individual tree structure construction, merged tree construction, and total construction time for jXBW, Ptree, SucTree, and Saxon. The construction time of jXBW, Ptree, and SucTree includes both individual tree structure construction time and merged tree construction time. The results demonstrate that jXBW's index construction time is competitive with other tree-based approaches, as merged tree construction dominates the overall time. While Saxon demonstrates faster construction times for most datasets due to its optimized XML parsing pipeline, jXBW's construction overhead is comparable to Ptree and SucTree. The construction process involves two phases: building individual tree structures and merging them into the final jXBW structure. This one-time construction cost is amortized over numerous queries, where jXBW's superior query performance provides substantial benefits.

The experimental results demonstrate that jXBW successfully addresses the key limitations of existing approaches. Unlike merged tree methods that suffer from exhaustive traversal overhead, jXBW's path decomposition strategy enables direct navigation to relevant positions. Compared to traditional succinct data structures that optimize for space at the expense of query time, jXBW achieves an optimal balance between memory efficiency and query performance. The consistent performance advantages across diverse datasets with varying structural complexities validate the effectiveness of jXBW for large-scale JSONL substructure search applications.

7.3 Case Study: Chemical Compound Analysis with GPT

To evaluate the effectiveness of our jXBW-based substructure search system in a real-world scientific context, we conducted a case study

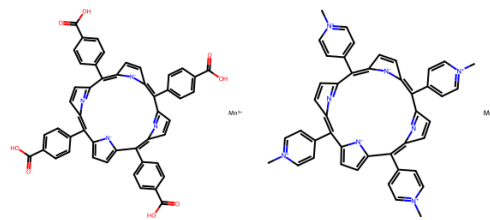


Figure 5: Representative molecular structures extracted from the PubChem dataset using jXBW-based substructure search with the query {"structure" : {"atoms" : [{"symbol" : "N", "charge" : 1}]}}. Left: Mn³⁺ porphyrin derivative with carboxyphenyl groups. Right: Pyridinium-substituted porphyrin complex. Both exhibit cationic nitrogen centers and are representative of structures with potential applications in photodynamic therapy and antimicrobial activity.

on a large-scale chemical compound dataset. Specifically, we used the pubchem dataset in Table 1. We performed a substructure search using the following query pattern:

```
{"structure" : {"atoms" : [{"symbol" : "N", "charge" : 1}]}}
```

This query targets compounds containing cationic nitrogen atoms (N⁺), a common structural motif found in quaternary ammonium salts, pyridinium derivatives, and metal–nitrogen complexes. Using our index, the search was executed in 21 milliseconds, significantly faster than Ptree (145 milliseconds) and SucTree (335 milliseconds). The search retrieved 838 compounds, from which 10 compounds were randomly selected for downstream analysis.

To investigate the biological and chemical implications of the retrieved structures, we provided these 10 compounds to GPT-4 and asked it to analyze their physicochemical features and predict possible pharmacological properties. The model identified a range of common traits, including:

- The frequent presence of quaternary or pyridinium-type nitrogen centers,
- Aromatic macrocycles resembling porphyrins,
- Multiple polar functional groups such as carboxyl and hydroxyl moieties,
- Coordination with transition metals (e.g., Mn³⁺, Ni³⁺).

GPT-4 inferred that these features significantly affect the electron distribution, aqueous solubility, and membrane permeability of the molecules. Based on this analysis, the compounds were suggested to exhibit potential as:

- Antimicrobial agents, due to their electrostatic interactions with negatively charged bacterial membranes,
- Photosensitizers for photodynamic therapy (PDT), enabled by their redox-active macrocyclic frameworks,
- DNA- or RNA-binding agents, given their positive charges and planar aromatic systems.

As illustrated in Figure 5, two representative compounds are shown. The left compound is a Mn³⁺-coordinated porphyrin derivative featuring carboxy-substituted phenyl groups, and the right

compound includes pyridinium-substituted porphyrin ligands. Both structures exemplify the combination of N^+ -based charge centers, extended conjugation, and potential redox activity, which GPT-4 highlighted as key factors for biological activity.

This case study highlights the synergy between our fast substructure search system and large language models. It demonstrates how the integration of symbolic querying with neural reasoning can accelerate early-stage compound triage, structure-function hypothesis generation, and drug discovery workflows.

8 CONCLUSION AND FUTURE WORK

This paper introduced jXBW, a novel approach for efficient substructure search on large-scale JSONL datasets. Our contributions address the fundamental limitations of existing methods through three key innovations: merged tree representation, succinct tree indexing based on the eXtended Burrows-Wheeler Transform, and path decomposition-based search algorithms.

Experimental evaluation across seven real-world datasets demonstrates significant performance improvements. jXBW consistently outperforms existing approaches, achieving performance gains ranging from $16\times$ for smaller datasets to $4,700\times$ for larger datasets compared to tree-based methods, and up to $6\text{ million}\times$ compared to XML-based processing. The case study with PubChem chemical compounds showcases the practical value of our approach in AI-powered scientific workflows, where fast retrieval enables seamless integration with large language models for compound analysis and drug discovery.

The success of jXBW opens several promising directions for future research. First, extending the path decomposition approach to support approximate substructure matching with edit distance constraints would enable more flexible query capabilities, particularly useful for handling noisy or incomplete data in real-world applications. This could leverage recent advances in approximate string matching on compressed indices. Second, investigating the applicability of our merged tree representation to other semi-structured data formats beyond JSON, such as protocol buffers, Apache Avro, and MessagePack, could broaden the impact of our techniques across diverse data ecosystems. Third, developing distributed versions of jXBW using consistent hashing and parallel query processing for extremely large datasets ($>100\text{GB}$) represents an important scalability challenge for next-generation Foundation Model training pipelines. Fourth, integrating semantic similarity measures with structural matching could enable AI-guided query expansion, where Foundation Models suggest structurally related patterns based on domain knowledge.

Finally, the integration of jXBW with foundation models demonstrated in our chemical compound case study suggests broader opportunities for symbolic-neural hybrid systems. Future work could explore how efficient structured data retrieval can enhance various AI applications, from prompt engineering and few-shot learning to knowledge-augmented generation and structured reasoning tasks.

REFERENCES

- [1] V Akhil. 2024. Border Crossing Entry Data. <https://www.kaggle.com/datasets/akhilv11/border-crossing-entry-data>. Dataset of border crossing entries.
- [2] Anthropic. 2023. Claude: A next-generation AI assistant based on Anthropic's research into training helpful, harmless, and honest AI systems. <https://www.anthropic.com/clause>. Accessed: 2024-12-01.
- [3] Saurabh Badole. 2024. Electric Vehicle Population Data. <https://www.kaggle.com/datasets/saurabhbhadole/electric-vehicle-population-data>. Dataset of electric vehicle registrations.
- [4] Rishi Bommasani, Drew A Hudson, Ehsan Adeli, Russ Altman, Sanjeev Arora, Sydney von Arx, Michael S Bernstein, Jeannette Bohg, Antoine Bosselut, Emma Brunskill, et al. 2021. On the opportunities and risks of foundation models. *arXiv preprint arXiv:2108.07258* (2021).
- [5] Tom Brown, Benjamin Mann, Nick Ryder, Melanie Subbiah, Jared D Kaplan, Prafulla Dhariwal, Arvind Neelakantan, Pranav Shyam, Girish Saxena, Ariel Mandel, et al. 2020. Language models are few-shot learners. *Advances in Neural Information Processing Systems* 33 (2020), 1877–1901.
- [6] Nicolas Bruno, Nick Koudas, and Divesh Srivastava. 2002. Holistic Twig Joins: Optimal XML Pattern Matching. In *Proceedings of the 2002 ACM SIGMOD International Conference on Management of Data*.
- [7] Ji Chen, Mu-Chun Huang, Guangzhi Xu, Sheng Liu, and Chi Wang. 2024. Does Prompt Formatting Have Any Impact on LLM Performance? *arXiv preprint arXiv:2411.10541* (2024).
- [8] Juhai Chen, Rifaa Qadri, Yuxin Wen, Neel Jain, John Kirchenbauer, Tianyi Zhou, and Tom Goldstein. 2024. GenQA: Generating Millions of Instructions from a Handful of Prompts. *arXiv:2406.10323 [cs.CL]* Available at <https://arxiv.org/abs/2406.10323>.
- [9] Francisco Claude, Gonzalo Navarro, and Alberto Ordóñez. 2012. The wavelet matrix. In *Proceedings of the 19th International Symposium on String Processing and Information Retrieval*. 167–179.
- [10] Jacob Devlin, Ming-Wei Chang, Kenton Lee, and Kristina Toutanova. 2018. BERT: Pre-training of Deep Bidirectional Transformers for Language Understanding. *arXiv preprint arXiv:1810.04805* (2018).
- [11] Paolo Ferragina, Raffaele Giancarlo, and Giovanni Manzini. 2009. The myriad virtues of Wavelet Trees. *Information and Computation* 207 (2009), 849–866.
- [12] Paolo Ferragina, Giovanni Manzini, Veli Mäkinen, and Gonzalo Navarro. 2007. Compressed representations of sequences and full-text indexes. In *Proceedings of the 18th Annual ACM-SIAM Symposium on Discrete Algorithms*. 636–645.
- [13] Simon Gog, Timo Beller, Alistair Moffat, and Matthias Petri. 2014. From Theory to Practice: Plug and Play with Succinct Data Structures. In *Proceedings of the 13th International Symposium on Experimental Algorithms*. 326–337. doi:10.1007/978-3-319-07959-2_28 SDSL-lite library available at <https://github.com/simongog/sdsl-lite>.
- [14] Roberto Grossi, Ankur Gupta, and Jeffrey Scott Vitter. 2003. High-order entropy-compressed text indexes. In *Proceedings of the 14th Annual ACM-SIAM Symposium on Discrete Algorithms*. SIAM, 841–850.
- [15] Guy Jacobson. 1989. Space-efficient static trees and graphs. In *Proceedings of the 30th Annual Symposium on Foundations of Computer Science*. IEEE, 549–554.
- [16] Michael Kay. 2024. Saxon XSLT and XQuery Processor. <https://www.saxonica.com/>. High-performance XQuery 3.1 and XSLT 3.0 processor.
- [17] Junhee Lee, Edman Anjos, and Srinivasa Rao Satti. 2020. SJSON: A succinct representation for JSON documents. *Information Systems* 97 (2020), 101686. doi:10.1016/j.is.2020.101686
- [18] Xiaoming Liu, Wei Zhang, and Yuxin Chen. 2021. Efficient Processing and Analysis of Large-Scale JSON Data in Modern Applications. *Electronics* 10 (2021), 621.
- [19] National Center for Biotechnology Information. 2024. PubChem Database. <https://pubchem.ncbi.nlm.nih.gov/>. Chemical compound database.
- [20] Gonzalo Navarro. 2012. Wavelet Trees for All. In *Proceedings of the 23rd Annual Symposium on Combinatorial Pattern Matching*. Vol. 7354. 2–26.
- [21] Gonzalo Navarro. 2016. *Compact data structures: a practical approach*. Cambridge University Press.
- [22] OpenStreetMap Contributors. 2024. OSM JSON Format. https://wiki.openstreetmap.org/wiki/OSM_JSON. OpenStreetMap geographical data in JSON format.
- [23] Mike Prust. 2024. Wikipedia Movie Data. <https://raw.githubusercontent.com/prust/wikipedia-movie-data/master/movies.json>. JSON dataset of movies scraped from Wikipedia.
- [24] Alec Radford, Jeffrey Wu, Rewon Child, David Luan, Dario Amodei, Ilya Sutskever, et al. 2019. Language models are unsupervised multitask learners. *OpenAI blog* 1, 8 (2019), 9.
- [25] Colin Raffel, Noam Shazeer, Adam Roberts, Katherine Lee, Sharan Narang, Michael Matena, Yanqi Zhou, Wei Li, and Peter J Liu. 2020. Exploring the limits of transfer learning with a unified text-to-text transformer. *The Journal of Machine Learning Research* 21, 1 (2020), 5485–5551.
- [26] A. D. Rau and M. Atique. 2014. A Survey of Indexing Techniques for XML Database. *COMPUSOFT: An International Journal of Advanced Computer Technology* 3 (2014), 461–466.
- [27] Hugo Touvron, Thibaut Lavril, Gautier Izacard, Xavier Martinet, Marie-Anne Lachaux, Timothée Lacroix, Baptiste Rozière, Naman Goyal, Eric Hambro, Faisal Azhar, et al. 2023. Llama: Open and efficient foundation language models. *arXiv preprint arXiv:2302.13971* (2023).

[28] Hugo Touvron, Louis Martin, Kevin Stone, Peter Albert, Amjad Almahairi, Yasmine Babaei, Nikolay Bashlykov, Soumya Batra, Prajwal Bhargava, Shruti Bhosale, et al. 2023. Llama 2: Open foundation and fine-tuned chat models. *arXiv preprint arXiv:2307.09288* (2023).

[29] U.S. Department of Transportation, Federal Transit Administration. 2024. Paratransit Data. <https://catalog.data.gov/dataset/?tags=paratransit>. Government dataset of paratransit services.

[30] Li Wang, Michael Brown, and Sarah Davis. 2022. Structured Data Formats for Large Language Model Training: A Comprehensive Analysis. *arXiv:2201.03051 [cs.CL]* Available at <https://arxiv.org/pdf/2201.03051>.

[31] Wei Zhang, Xiaoming Li, Yufei Chen, Jiahao Wang, and Pengfei Liu. 2025. Enhancing structured data generation with GPT-4o: evaluating prompt strategies for JSON, YAML, and hybrid CSV outputs. *Frontiers in Artificial Intelligence* 8 (2025), 1558938.

A TREE MERGING ALGORITHM

The pseudo code of **MergeTrees** is shown in Algorithm 2.

Algorithm 2 MergeTrees algorithm for merging two trees T and T' .

```

1: function MERGETREES( $T, T'$ )
2:   if  $T'$  has no nodes then
3:     return  $T$ 
4:   end if
5:   if  $T$  has no nodes then
6:      $T \leftarrow \text{COPYTREE}(T')$             $\triangleright$  Copy entire tree structure
7:     return  $T$ 
8:   end if
9:   if  $T.\text{root}.label \neq T'.\text{root}.label$  then
10:    ADDSUBTREE( $T.\text{root}, T'.\text{root}$ )     $\triangleright$  Add the tree  $T'$  as a
      new child of the root of  $T$ 
11:   else                                 $\triangleright$  Same root labels
12:     MERGERECURSIVE( $T.\text{root}, T'.\text{root}$ )   $\triangleright$  Merge the trees
      recursively
13:   end if
14:   return  $T$ 
15: end function
16: function MERGERECURSIVE( $node, node'$ )
17:   if  $node'$  is leaf then            $\triangleright$  Merge tree IDs from leaf node
18:      $node.\text{ids} \leftarrow node.\text{ids} \cup node'.\text{ids}$ 
19:     return
20:   end if
21:   for each  $child'$  in  $node'.\text{children}$  do
22:      $found \leftarrow \text{false}$ 
23:     for each  $child$  in  $node.\text{children}$  do
24:       if  $child.\text{label} = child'.\text{label}$  then
25:         MERGERECURSIVE( $child, child'$ )
26:          $found \leftarrow \text{true}$ 
27:         break
28:       end if
29:     end for
30:     if  $found = \text{false}$  then       $\triangleright$  No matching child found
31:       ADDSUBTREE( $node, child'$ )  $\triangleright$  Add the subtree to the
      node as a new child
32:     end if
33:   end for
34: end function
35: function ADDSUBTREE( $parent, node'$ )
36:   Create a new node  $new\_node$  with label  $node'.\text{label}$ 
37:    $new\_node.\text{ids} \leftarrow node'.\text{ids}$ 
38:    $parent.\text{children} \leftarrow parent.\text{children} \cup \{new\_node\}$ 
39:   for each  $child'$  in  $node'.\text{children}$  do
40:     ADDSUBTREE( $new\_node, child'$ )
41:   end for
42: end function

```

B MERGED TREE SUBSTRUCTURE SEARCH ALGORITHMS

This appendix provides the detailed algorithms for substructure search on merged tree as described in Section 3.1.

Algorithm 3 SubstructureSearch algorithm on merged tree for finding all tree identifiers of trees T_i that contain query tree Q as a subtree.

```

1: function SUBSTRUCTURESEARCHMT( $MT, Q$ )
2:    $solutions \leftarrow \emptyset$ 
3:    $root\_label \leftarrow$  label of root node in  $Q$ 

          ▷ Step 1: Candidate Finding
4:    $candidates \leftarrow \text{FINDCANDIDATENODES}(MT, root\_label)$ 

          ▷ Step 2: Substructure Matching
5:   for each  $candidate \in candidates$  do
6:      $leaf\_id\_sets \leftarrow \text{MATCHSUBTREE}(candidate, Q.root)$ 
7:     if  $leaf\_id\_sets \neq \emptyset$  then
          ▷ Step 3: Solution Identification
8:        $intersection\_ids \leftarrow \bigcap_{ids \in leaf\_id\_sets} ids$ 
9:        $solutions \leftarrow solutions \cup intersection\_ids$ 
10:    end if
11:   end for
12:   return  $solutions$ 
13: end function

```

Algorithm 4 FindCandidateNodes algorithm for finding all nodes in merged tree with specified label.

```

1: function FINDCANDIDATENODES( $MT, root\_label$ )
2:    $candidates \leftarrow \emptyset$ 
3:   TRAVERSEMT( $MT.root, root\_label, candidates$ )
4:   return  $candidates$ 
5: end function

6: function TRAVERSEMT( $node, target\_label, candidates$ )
7:   if  $node.label = target\_label$  then
8:      $candidates \leftarrow candidates \cup \{node\}$ 
9:   end if
10:  for each  $child \in node.children$  do
11:    TRAVERSEMT( $child, target\_label, candidates$ )
12:  end for
13: end function

```

Algorithm 5 MatchSubtree algorithm for matching subtree structure with root mt_node against query tree with root q_node .

```

1: function MATCHSUBTREE( $mt\_node, q\_node$ )
2:   if both  $q\_node$  and  $mt\_node$  are leaf then
3:     return  $\{mt\_node.ids\}$ 
4:   else if  $q\_node$  is leaf and  $mt\_node$  is not leaf then
5:     return  $\emptyset$ 
6:   else if  $q\_node$  is not leaf and  $mt\_node$  is leaf then
7:     return  $\emptyset$ 
8:   end if
          ▷ Both nodes are internal: match children in order
9:    $all\_leaf\_ids \leftarrow \emptyset$ 
10:   $mt\_idx \leftarrow 1, q\_idx \leftarrow 1$ 
11:  while  $q\_idx \leq |q\_node.children|$  and  $mt\_idx \leq |mt\_node.children|$  do
12:     $q\_child \leftarrow q\_node.children[q\_idx]$ 
13:     $mt\_child \leftarrow mt\_node.children[mt\_idx]$ 
14:    if  $mt\_child.label = q\_child.label$  then
15:       $result \leftarrow \text{MATCHSUBTREE}(mt\_child, q\_child)$ 
16:      if  $result \neq \emptyset$  then
17:         $all\_leaf\_ids \leftarrow all\_leaf\_ids \cup result$ 
18:         $q\_idx \leftarrow q\_idx + 1$ 
19:      else
20:        return  $\emptyset$ 
21:      end if
22:    end if
23:     $mt\_idx \leftarrow mt\_idx + 1$ 
24:  end while
25:  if  $q\_idx \leq |q\_node.children|$  then
26:    return  $\emptyset$  ▷ Some query children were not matched
27:  end if
28:  return  $all\_leaf\_ids$ 
29: end function

```

C XBW OPERATIONS: DETAILED ALGORITHMS AND EXAMPLES

This appendix provides detailed algorithms, implementation specifics, and worked examples for the five XBW operations introduced in Section 5.2.

C.1 Children Operation

Children(i): The core idea exploits the XBW property that siblings are contiguously aligned in the arrays. We identify the label at position i (which becomes the parent label for the children we seek), locate the first occurrence of nodes having this parent label, and then use the binary encoding in A_{last} to determine the exact range where all children of position i are stored. The algorithm is computed as follows: (i) Compute the character c at position i in A_{label} using the access operation $\text{access}(A_{label}, i)$ on the wavelet matrix. (ii) $F(c)$ returns the first position y such that the parent of the node at y has label c . This is computed by constructing an array A_{pf} where $A_{pf}[j]$ equals the first character of $A_{anc}[j]$ if $j \neq 1$ and $A_{pf}[j] = 0$ otherwise; $F(c)$ is computed as $\text{select}_c(A_{pf}, 1)$. (iii) The children range $[l, r]$ is then determined using rank and select operations on A_{last} to find the contiguous block of siblings as

follows: $l = \text{select}_1(A_{last}, z+s-1) + 1$ and $r = \text{select}_1(A_{last}, z+s)$, where $z = \text{rank}_1(A_{last}, y)$ and $s = \text{rank}_c(A_{label}, i)$.

The pseudo code of **Children**(i) is shown in Algorithm 6.

Algorithm 6 Children algorithm for retrieving the range of children for the entry at position i in the XBW representation.

```

1: function CHILDREN( $i$ )
2:    $c \leftarrow \text{access}(A_{label}, i)$             $\triangleright$  Label of the potential parent
3:    $y \leftarrow F(c)$   $\triangleright$  First position whose ancestor prefix starts with
   label  $c$ 
4:    $z \leftarrow \text{rank}_1(A_{last}, y)$             $\triangleright$  Number of 1s up to position  $y$ 
5:    $s \leftarrow \text{rank}_c(A_{label}, i)$   $\triangleright$  Number of occurrences of label  $c$  up
   to position  $i$ 
6:    $l \leftarrow \text{select}_1(A_{last}, z+s-1) + 1$   $\triangleright$  Start of children block
7:    $r \leftarrow \text{select}_1(A_{last}, z+s)$             $\triangleright$  End of children block
8:   return  $[l, r]$                             $\triangleright$  Range of child entries
9: end function

```

Example: An example of **Children**(i) for $i = 5$ on the XBW in Fig. 4(V) is as follows: (i) Compute $c = \text{access}(A_{label}, 5) = I$. (ii) Compute $y = F(I) = 11$, where position 11 is the first position with parent node label I . (iii) Compute $z = \text{rank}_1(A_{last}, y) = \text{rank}_1(A_{last}, 11) = 6$ and $s = \text{rank}_I(A_{label}, i) = \text{rank}_I(A_{label}, 5) = 1$. (iv) Compute $l = \text{select}_1(A_{last}, z+s-1)+1 = \text{select}_1(A_{last}, 6)+1 = 11$ and $r = \text{select}_1(A_{last}, z+s) = \text{select}_1(A_{last}, 7) = 12$. (v) The children range is $[11, 12]$.

C.2 RankedChild and CharRankedChild Operations

Both **RankedChild**(i, k) and **CharRankedChild**(i, c, k) utilize the starting position l from the range $[l, r] = \text{Children}(i)$. **RankedChild** is computed as $l + k - 1$. **CharRankedChild**(i, c, k) is computed as follows: (i) Compute $y = \text{rank}_c(A_{label}, l-1)$ to obtain the number of occurrences of c up to position $l-1$; (ii) Compute $p = \text{select}_c(A_{label}, y+k)$ to find the $(y+k)$ -th occurrence position of c in A_{label} .

C.3 Parent Operation

Parent(i): The key idea is to leverage the lexicographic ordering of the XBW representation. Since nodes with the same ancestor paths are grouped together, we can identify the group containing position i , determine how many sibling groups with the same parent have been completed, and use this information to locate the parent's position. The algorithm is computed as follows: (i) Compute $s = \text{rank}_1(A_{diff}, i)$, where A_{diff} is a binary array: $A_{diff}[i] = 1$ iff $A_{anc}[i] \neq A_{anc}[i-1]$ for $i \neq 1$; $A_{diff}[1] = 1$. For example in Fig. 4, $A_{diff} = [1, 1, 0, 1, 0, 1, 1, 0, 1, 1, 1, 0]$. The value s gives the number of distinct sequences appearing up to position i in the array. (ii) Compute $y = \text{select}_1(A_{diff}, s)$, which gives the starting position of the group in A_{label} that shares the same first label of ancestor sequences in A_{anc} at position i . (iii) Compute $c = \text{access}(A_{pf}, i)$. The character c corresponds to the label of the parent node at position i . (iv) Compute $k = \text{rank}_1(A_{last}, i) - \text{rank}_1(A_{last}, y)$, which represents the number of sibling groups with parent label c that have completed between positions y and i . (v) The position of the

parent is then determined as $p = \text{select}_c(A_{label}, k+1)$, which gives the position of the $(k+1)$ -th occurrence of label c in A_{label} (the $+1$ accounts for the parent position relative to the sibling group count). (vi) Return p as the position corresponding to the parent of the node at position i .

The pseudo code of **Parent**(i) is shown in Algorithm 7.

Algorithm 7 Parent algorithm for retrieving the parent position of the entry at position i in the XBW representation.

```

1: function PARENT( $i$ )
2:   if  $i = 0$  then
3:     return NULL            $\triangleright$  Root node has no parent
4:   end if
5:    $s \leftarrow \text{rank}_1(A_{diff}, i)$             $\triangleright$  Number of distinct ancestor
   prefixes up to  $i$ 
6:    $y \leftarrow \text{select}_1(A_{diff}, s)$             $\triangleright$  Start position of the group
   containing  $i$ 
7:    $c \leftarrow \text{access}(A_{pf}, i)$             $\triangleright$  Parent label of entry at position  $i$ 
8:    $k \leftarrow \text{rank}_1(A_{last}, i) - \text{rank}_1(A_{last}, y)$             $\triangleright$  Sibling group
   index
9:    $p \leftarrow \text{select}_c(A_{label}, k+1)$   $\triangleright$   $(k+1)$ -th occurrence of label  $c$ 
10:  return  $p$                             $\triangleright$  Parent position in  $A_{label}$ 
11: end function

```

Example: An example of **Parent**(i) for $i = 5$ on the XBW in Fig. 4(V) is as follows: (i) Compute $s = \text{rank}_1(A_{diff}, i) = \text{rank}_1(A_{diff}, 5) = 3$. (ii) Compute $y = \text{select}_1(A_{diff}, s) = \text{select}_1(A_{diff}, 3) = 4$. (iii) Compute $c = \text{access}(A_{pf}, i) = \text{access}(A_{pf}, 5) = A$. (iv) Compute $k = \text{rank}_1(A_{last}, i) - \text{rank}_1(A_{last}, y) = \text{rank}_1(A_{last}, 5) - \text{rank}_1(A_{last}, 4) = 2 - 1 = 1$. (v) Compute $p \leftarrow \text{select}_A(A_{label}, k+1) = \text{select}_A(A_{label}, 2) = 9$. (vi) Return $p = 9$ as the position corresponding to the parent of the node at position $i = 5$.

C.4 SubPathSearch Operation

SubPathSearch(P): The key idea is to iteratively narrow down the range of positions in A_{label} by processing each label in the path $P = \langle p_1, p_2, \dots, p_k \rangle$ sequentially. Starting with nodes that have the first label p_1 , we progressively refine the search range to find nodes reachable through the specified path. The algorithm is computed as follows: (i) If the path P is empty, return the range $[0, |MT| - 1]$. (ii) For the first label p_1 , compute the initial range $[\text{first}, \text{last}]$ using the F-array: $\text{first} = F(p_1)$ and $\text{last} = F(p_1 + 1) - 1$, where $F(c)$ gives the first position of nodes whose parent has label c . (iii) For each subsequent label p_i ($i = 2, 3, \dots, |P|$), refine the current range $[\text{first}, \text{last}]$ by: (a) Computing $k_1 = \text{rank}_{p_i}(A_{label}, \text{first} - 1)$ and $k_2 = \text{rank}_{p_i}(A_{label}, \text{last})$ to count occurrences of p_i within the current range. (b) Computing the positions $z_1 = \text{select}_{p_i}(A_{label}, k_1 + 1)$ and $z_2 = \text{select}_{p_i}(A_{label}, k_2)$ to find the first and last occurrences of p_i within the range. (c) If $i = |P|$ (final label), set $\text{first} = z_1$ and $\text{last} = z_2$ and terminate. (d) Otherwise, update the range to the children of the matched nodes: $\text{first} = \text{RankedChild}(z_1, 1)$ and $\text{last} = \text{RankedChild}(z_2, \text{degree}(z_2))$. Here, $\text{degree}(z_2)$ is the number of children of the node at position z_2 , computed as $r - l + 1$ where $[l, r]$ is the range computed by **Children**(z_2). (iv) Return

Algorithm 8 SubPathSearch algorithm for finding nodes that match a path $P = \langle p_1, p_2, \dots, p_k \rangle$ on jXBW.

```

1: function SUBPATHSEARCH( $P$ )
2:   if  $P$  is empty then
3:     return  $[0, |MT| - 1]$                                  $\triangleright$  Match all entries
4:   end if
5:    $first \leftarrow F(p_1)$ 
6:    $last \leftarrow F(p_1 + 1) - 1$ 
7:   if  $first > last$  then
8:     return NULL                                      $\triangleright$  No match found
9:   end if
10:  for  $i = 2$  to  $|P|$  do
11:     $c \leftarrow p_i$ 
12:     $k_1 \leftarrow \text{rank}_c(A_{label}, first - 1)$ 
13:     $k_2 \leftarrow \text{rank}_c(A_{label}, last)$ 
14:    if  $k_2 \leq k_1$  then
15:      return NULL                                      $\triangleright$  No match in range
16:    end if
17:     $z_1 \leftarrow \text{select}_c(A_{label}, k_1 + 1)$ 
18:     $z_2 \leftarrow \text{select}_c(A_{label}, k_2)$ 
19:    if  $i = |P|$  then
20:      return  $[z_1, z_2]$                                  $\triangleright$  Final range
21:    end if
22:     $first \leftarrow \text{RankedChild}(z_1, 1)$ 
23:     $last \leftarrow \text{RankedChild}(z_2, \text{degree}(z_2))$ 
24:    if  $first = \text{NULL}$  or  $last = \text{NULL}$  then
25:      return NULL                                      $\triangleright$  Invalid child range
26:    end if
27:  end for
28:  return  $[first, last]$ 
29: end function

```

the final range $[first, last]$ representing positions of nodes that are reachable through path P .

The pseudo code of **SubPathSearch**(P) is shown in Algorithm 8.

D HELPER ALGORITHMS FOR SUBSTRUCTURE SEARCH

This appendix provides the detailed implementations of the helper function used by the SubstructureSearch algorithm.

D.1 ComputeAncestors Algorithm

Algorithm 9 ComputeAncestors algorithm for collecting ancestor positions that are $|P| - 1$ levels up from positions in range $[first, last]$ for path P on jXBW.

```

1: function COMPANCESTORS( $[first, last], P$ )
2:    $ancestor\_set \leftarrow$  empty set
3:    $path\_length \leftarrow |P|$ 
4:   for each position  $i$  from  $first$  to  $last$  do
5:      $pos \leftarrow i$ 
6:     for  $j = 1$  to  $path\_length - 1$  do     $\triangleright$  Trace back  $|P| - 1$ 
levels
7:        $pos \leftarrow \text{PARENT}(pos)$ 
8:     end for
9:     if  $pos$  is not in  $ancestor\_set$  then
10:       $ancestor\_set \leftarrow ancestor\_set \cup \{pos\}$    $\triangleright$  Add new
ancestor
11:    end if
12:  end for
13:  return  $ancestor\_set$ 
14: end function

```

D.2 CollectPathMatchingIDs Algorithm

Algorithm 10 CollectPathMatchingIDs algorithm for collecting tree identifiers from leaf nodes of paths starting from a validated subtree root position *root_pos* and matching query root-to-leaf paths.

```

1: function COLLECTPATHMATCHINGIDS(root_pos, paths)
2:   sets_of_ids  $\leftarrow$  empty list
3:   for each path in paths do
4:     path_leaf_ids  $\leftarrow$  empty set
5:     current_positions  $\leftarrow$   $\{root\_pos\}$             $\triangleright$  Start with
       matching subtree root position
6:     for each label in path do
7:       next_positions  $\leftarrow$  empty set
8:       for each current in current_positions do
9:         k  $\leftarrow$  1
10:        while CHARRANKEDCHILD(current, label, k)  $\neq$ 
        NULL do
11:          child                                 $\leftarrow$ 
          CHARRANKEDCHILD(current, label, k)
12:          next_positions  $\leftarrow$  next_positions  $\cup$   $\{child\}$ 
13:          k  $\leftarrow$  k + 1
14:        end while
15:      end for
16:      current_positions  $\leftarrow$  next_positions
17:      if current_positions is empty then
18:        break            $\triangleright$  No matching children found
19:      end if
20:    end for
        $\triangleright$  Collect tree IDs from all matching leaf positions
21:    for each leaf_pos in current_positions do
22:      leaf_ids  $\leftarrow$  A_ids[rank1(Aleaf, leaf_pos)]
23:      path_leaf_ids  $\leftarrow$  path_leaf_ids  $\cup$  leaf_ids
24:    end for
25:    if path_leaf_ids is empty then
26:      return  $\emptyset$      $\triangleright$  Early termination if any path fails
27:    end if
28:    sets_of_ids  $\leftarrow$  sets_of_ids  $\cup$   $\{path\_leaf\_ids\}$ 
29:  end for
30: return sets_of_ids
31: end function

```

D.3 Structural Matching Algorithm

Algorithm 11 StructMatch algorithm for collecting sets of tree identifiers from leaf nodes by directly matching query tree structure while preserving array ordering constraints.

```

1: function STRUCTMATCH(cur_pos, query_node)     $\triangleright$  Check if
   current position's label matches query node's label
2:   if ACCESS(Alabel, cur_pos)  $\neq$  query_node.label then
3:     return  $\emptyset$            $\triangleright$  Label mismatch: no matching trees
4:   end if
5:   if query_node is leaf then
6:     return {TREEIDS(cur_pos)}     $\triangleright$  Base case: return set
       containing tree IDs from leaf
7:   end if
8:   q_children  $\leftarrow$  query_node.children
9:   if query_node is JSON array then
10:    return ARRAYMATCH(cur_pos, q_children)
11:   else            $\triangleright$  Unordered matching (JSON object or general
       subtree)
12:    return OBJECTMATCH(cur_pos, q_children)
13:   end if
14: end function

```

Algorithm 12 ArrayMatch algorithm for collecting sets of tree identifiers by matching JSON array elements as consecutive subsequences while preserving ordering constraints.

```

1: function ARRAYMATCH(cur_pos, q_children)
2:   result_tree_ids  $\leftarrow$   $\emptyset$ 
3:   [child_start, child_end]  $\leftarrow$  CHILDREN(cur_pos)     $\triangleright$  Get
   range of child positions
4:   num_children  $\leftarrow$  child_end - child_start + 1
5:   query_length  $\leftarrow$  |q_children|
6:   if num_children < query_length then
7:     return  $\emptyset$   $\triangleright$  Not enough children to match query array
8:   end if
        $\triangleright$  Use CharRankedChild for efficient label-based matching
9:   id_sets  $\leftarrow$ 
10:  RECURSIVEARRAYMATCH(cur_pos, q_children, 1, 0)
11:  return id_sets
12: end function

```

Algorithm 13 RecursiveArrayMatch algorithm for collecting sets of tree identifiers through efficient array subsequence matching using CharRankedChild.

```

1: function RECURSIVEARRAYMATCH(cur_pos, q_children, q_idx,  

   min_pos)
2:   if q_idx > |q_children| then
3:     return  $\emptyset$   $\triangleright$  All query elements matched successfully,  

   return empty set of sets
4:   end if
5:   result_tree_ids  $\leftarrow \emptyset
6:   target_label  $\leftarrow q\_children[q\_idx].label$ 
7:   k  $\leftarrow 1$ 
       $\triangleright$  Find all children with target label using
      CharRankedChild
8:   while CHARRANKEDCHILD(cur_pos, target_label, k)  $\neq$ 
      NULL do
9:     child_pos  $\leftarrow$ 
10:    CHARRANKEDCHILD(cur_pos, target_label, k)
         $\triangleright$  Check ordering constraint: must be after previous
        match
11:    if child_pos  $\leq$  min_pos then
12:      k  $\leftarrow k + 1$ 
13:      continue  $\triangleright$  Skip positions that violate ordering
14:    end if
         $\triangleright$  Match current query element at this position
15:    current_ids  $\leftarrow$ 
16:    STRUCTMATCH(child_pos, q_children[q_idx])
17:    if current_ids  $\neq \emptyset$  then  $\triangleright$  Recursively match
      remaining elements with updated minimum position
18:      remaining_id_sets  $\leftarrow$ 
19:      RECURSIVEARRAYMATCH(cur_pos, q_children, q_idx +  

      1, child_pos)  $\triangleright$  Combine current IDs with remaining ID sets
20:      result_tree_ids  $\leftarrow$  result_tree_ids  $\cup$   

      {current_ids}  $\cup$  remaining_id_sets
21:    end if
22:    k  $\leftarrow k + 1$ 
23:  end while
24:  return result_tree_ids
25: end function$ 
```

Algorithm 14 ObjectMatch algorithm for collecting sets of tree identifiers by matching JSON object key-value pairs without ordering constraints.

```

1: function OBJECTMATCH(cur_pos, q_children)
2:   child_id_sets  $\leftarrow \emptyset$   $\triangleright$  Collect sets of tree IDs for each child
   query
3:   for each child_query in q_children do
4:     child_tree_ids  $\leftarrow \emptyset
5:     label  $\leftarrow child\_query.label$ 
6:     k  $\leftarrow 1$ 
         $\triangleright$  Find all children with matching label
7:     while CHARRANKEDCHILD(cur_pos, label, k)  $\neq$  NULL
      do
8:       child_pos  $\leftarrow$ 
9:       CHARRANKEDCHILD(cur_pos, label, k)
10:      subtree_ids  $\leftarrow$  STRUCTMATCH(child_pos, child_query)
11:      child_tree_ids  $\leftarrow$  child_tree_ids  $\cup$  subtree_ids
12:      k  $\leftarrow k + 1$ 
13:    end while
         $\triangleright$  Collect the set of tree IDs for this child query
14:    child_id_sets  $\leftarrow$  child_id_sets  $\cup$  {child_tree_ids}
15:  end for
16:  return child_id_sets
17: end function$ 
```

Received 31 July 2025; revised XXX XXX XXX; accepted XXX XXX XXX